JOURNAL OF GUIDANCE, CONTROL, AND DYNAMICS
Vol. 21, No. 3, May–June 1998

Satellite Angular Rate Estimation from Vector Measurements

Ruth Azor*
Israel Aircraft Industries, Inc., Yehud, Industrial Zone 56000, Israel
Itzhack Y. Bar-Itzhack†
Technion—Israel Institute of Technology, 32000 Haifa, Israel
and
Richard R. Harman‡
NASA Goddard Space Flight Center, Greenbelt, Maryland 20771

An algorithm is presented for estimating the angular rate vector of a satellite that is based on the time derivatives of vector measurements expressed in a reference and in body coordinates. The computed derivatives are fed into a special Kalman filter, which yields an estimate of the spacecraft angular velocity. This filter, an extended interlaced Kalman filter (EIKF), is an extension of the interlaced Kalman filter (IKF) presented in the literature. Like the IKF, the EIKF is a suboptimal Kalman filter that, although being linear, estimates the state of a nonlinear dynamic system. It consists of two or three parallel Kalman filters whose individual estimates are fed to one another and are considered as known inputs by the other parallel filter(s). The nonlinear dynamics stem from the nonlinear differential equation that describes the rotation of a three-dimensional body. Tests using simulated as well as real Rossi X-Ray Timing Explore satellite data indicate that the algorithm works satisfactorily.

Nomenclature

$\boldsymbol{b}$	= vector measured by an attitude sensor such as a sun sensor, horizon sensor, etc.
$[\boldsymbol{b}\times]$	= cross product matrix of measured vector $\boldsymbol{b}$
D_b^i	= transformation matrix from i to b
$G^{\#}$	= pseudoinverse of G
$\boldsymbol{h}$	= angular momentum of the reaction or the momentum wheels
I	= moment of inertia tensor
I_{xx}, I_{yy}, I_{zz}	= moments of inertia about the body major axes x, y, and z, respectively
I_{xy}, I_{xz}, I_{yz}	= product moment of inertia terms
$\boldsymbol{n}$	= white noise vector
T	= external torque applied to the spacecraft
$\boldsymbol{v}$	= white noise vector
$\boldsymbol{\omega}$	= angular rate vector
$\hat{\boldsymbol{\omega}}$	= estimate of ω

Superscripts

T	= transpose
$\cdot$	= time differentiation

I. Introduction

SMALL inexpensive satellites that do not carry gyroscopes onboard still need the angular rate vector for attitude determination and for control loop damping. The same necessity also exists in gyro equipped satellites when performing high-rate maneuvers whose angular rate is out of range of the onboard gyros. Whereas the attitude determination task requires high-precision angular rate measurements, low-precision angular rate measurements are usually adequate for control loop damping. Satellites usually utilize vector measurements for attitude determination. Such measurements are, for example, the direction of the nadir, of the sun, of the magnetic field vector, etc. The vector measurements can be differentiated in time to obtain valuable information. This approach was used by Natanson[1] for estimating attitude from magnetometer measurements and by Challa et al.[2] to obtain attitude as well as rate.

Angular rate can be extracted from vector measurements in the following way. For the time being let us assume that $\boldsymbol{b}$ is the Earth magnetic field vector. From the laws of dynamics it is known that

$$\dot{\boldsymbol{b}}^i = \dot{\boldsymbol{b}}^b + \boldsymbol{\omega} \times \boldsymbol{b} \tag{1}$$

where $\dot{\boldsymbol{b}}^i$ is the time derivative of $\boldsymbol{b}$ as seen by an observer in inertial coordinates i, $\dot{\boldsymbol{b}}^b$ is the time derivative of $\boldsymbol{b}$ as seen by an observer in body coordinates b, and $\boldsymbol{\omega}$ is the angular rate vector of coordinate system b with respect to coordinate system i. (Note that the choice of the inertial coordinate system as the reference coordinates is arbitrary.) We can write Eq. (1) as follows:

$$[\boldsymbol{b}\times]\boldsymbol{\omega} = \dot{\boldsymbol{b}}^b - \dot{\boldsymbol{b}}^i \tag{2a}$$

Note that $\dot{\boldsymbol{b}}^i$ is computable because $\boldsymbol{b}$ is usually known from Almanac or a model, and $\dot{\boldsymbol{b}}^b$ is computable from the measurements. Consequently, all elements of Eq. (2a) other than ω are known. Let us resolve Eq. (2a) in the body coordinates then Eq. (2a) can be written as

$$[\boldsymbol{b}\times]\boldsymbol{\omega} = \dot{\boldsymbol{b}} - D_b^i \dot{\boldsymbol{b}}^i \tag{2b}$$

where the dot denotes a simple time derivative with respect to the b frame. Note that $\dot{\boldsymbol{b}}^i$ is resolved in the i coordinates and D_b^i has to be known. We realize that $\boldsymbol{\omega}$ cannot be determined from Eq. (2b) because $[\boldsymbol{b}\times]$ is not invertible. If we add one more vector measurement $\boldsymbol{c}$ from an additional sensor, however, then $\boldsymbol{\omega}$ can be determined as shown next. Similarly to Eq. (2b), we can write for $\boldsymbol{c}$

$$[\boldsymbol{c}\times]\boldsymbol{\omega} = \dot{\boldsymbol{c}} - D_b^i \dot{\boldsymbol{c}}^i \tag{3}$$

When we augment Eqs. (2b) and (3) into one equation we obtain

$$\begin{bmatrix} \dot{\boldsymbol{b}} - D_b^i \dot{\boldsymbol{b}}^i \\ \cdots\cdots \\ \dot{\boldsymbol{c}} - D_b^i \dot{\boldsymbol{c}}^i \end{bmatrix} = \begin{bmatrix} 0 & -b_z & b_y \\ b_z & 0 & -b_x \\ -b_y & b_x & 0 \\ 0 & -c_z & c_y \\ c_z & 0 & -c_x \\ -c_y & c_x & 0 \end{bmatrix} \begin{bmatrix} \omega_x \\ \omega_y \\ \omega_z \end{bmatrix} \tag{4}$$

Presented as Paper 96-3751 at the AIAA Guidance, Navigation, and Control Conference, San Diego, CA, July 29–31, 1996; received Jan. 21, 1997; revision received Oct. 20, 1997; accepted for publication Oct. 24, 1997.

*Senior Control Engineer, Systems and Space Technology, Electronics Division, MBT, Systems Engineering Department.

†Sophie and William Shamban Professor of Aerospace Engineering, Faculty of Aerospace Engineering, and Member, Technion Space Research Institute. Associate Fellow AIAA.

‡Aerospace Engineer, Flight Mechanics Branch, Code 552.

Define

$$\boldsymbol{d} = \begin{bmatrix} \dot{\boldsymbol{b}} - D_b^i \dot{\boldsymbol{b}}^i \\ \cdots\cdots \\ \dot{\boldsymbol{c}} - D_b^i \dot{\boldsymbol{c}}^i \end{bmatrix} \tag{5a}$$

$$G = \begin{bmatrix} 0 & -b_z & b_y \\ b_z & 0 & -b_x \\ -b_y & b_x & 0 \\ 0 & -c_z & c_y \\ c_z & 0 & -c_x \\ -c_y & c_x & 0 \end{bmatrix} \tag{5b}$$

$$\boldsymbol{\omega} = \begin{bmatrix} \omega_x \\ \omega_y \\ \omega_z \end{bmatrix} \tag{5c}$$

then Eq. (4) can be written as

$$\boldsymbol{d} = G\boldsymbol{\omega} \tag{6}$$

Next, define $G^{\#}$ as follows[3]:

$$G^{\#} = (G^T G)^{-1} G^T \tag{7}$$

then $\hat{\boldsymbol{\omega}}$ is given by

$$\hat{\boldsymbol{\omega}} = G^{\#}\boldsymbol{d} \tag{8}$$

Note that this solution exists only if $\boldsymbol{b}$ and $\boldsymbol{c}$ are not colinear.

An estimate of $\boldsymbol{\omega}$, better than that given in Eq. (8), can be obtained when the problem is treated as a stochastic problem and some kind of filtering is applied to the measurements. Moreover, filtering in the sense of estimation is a must when at each time point we have only one vector measurement. (Such a case exists, for example, when we use a sun sensor and some other vector measuring sensor, and the satellite happens to be in a shadowed zone.) In such a case we use the vehicle dynamics for propagating the estimate of $\boldsymbol{\omega}$. As will be shown in the ensuing, the dynamics model of a spacecraft (SC) is a nonlinear model; therefore, a linear Kalman filter (KF) is not suitable, and some kind of a nonlinear estimator is needed for estimating $\boldsymbol{\omega}$. The extended KF (EKF) is, then, the natural choice. However, Algrain and Saniie[4] and Algrain and Ehlers[5] introduced the interlaced KF (IKF), which is a suboptimal filter that is a combination of two linear KFs that operate simultaneously and feed one another. Their work motivated us to examine the latter approach rather than the EKF, which is known to have a convergence problem in certain cases. The IKF of Algrain and Saniie[4] is an ingenious idea. In their application, they fed the filter with the angular rate vector itself as measured by gyros and not with vector-derivative information. Essentially, they used the IKF as a low-pass filter and not as an estimator. This is equivalent to using the IKF for filtering $\hat{\boldsymbol{\omega}}$ computed in Eq. (8).

In contrast to Algrain and Saniie,[4] we use their idea to estimate the angular rate vector directly from vector measurements and their time derivatives and are able to obtain estimates even when we have a single measurement at each time point. We also extend their dynamics model further to include products of inertia. This leads to the use of two or three more sophisticated KFs that make use of three dynamics models. We call the extended filter the extended IKF (EIKF). Finally, our work differs considerably from that of Natanson[1] and Challa et al.[2] mainly because most of our investigation is dedicated to the filtering stage.

In the next section, we develop the dynamics models that give rise to the use of the EIKF. This leads to the development in Sec. III of measurement equations that correspond to the states of the dynamic models. In Sec. IV we present the stochastic models that are used by the EIKF. They are based on the dynamics and measurement models derived in Secs. II and III, respectively. Then, in Sec. V we introduce several options for implementing the EIKF followed by test results of the EIKF, which we show in Sec. VI. Finally, in Sec. VII we present our conclusions.

II. SC Dynamics

To apply a recursive estimator to estimate the angular rate vector of a gyroless SC, one needs to utilize the dynamics model of the SC. The angular dynamics of an SC are given in the following equation[6]:

$$I\dot{\boldsymbol{\omega}} + \dot{\boldsymbol{h}} + \boldsymbol{\omega} \times (I\boldsymbol{\omega} + \boldsymbol{h}) = \boldsymbol{T} \tag{9}$$

where $\boldsymbol{\omega}$ is the angular velocity of the satellite with respect to inertial space. All of the vectors in Eq. (9) are expressed in body coordinates. Because I is nonsingular, we may write Eq. (9) as

$$\dot{\boldsymbol{\omega}} = -I^{-1}[\boldsymbol{\omega} \times (I\boldsymbol{\omega} + \boldsymbol{h})] + I^{-1}(\boldsymbol{T} - \dot{\boldsymbol{h}}) \tag{10}$$

The inertia matrix I is given by[7]

$$I = \begin{bmatrix} I_{xx} & -I_{xy} & -I_{xz} \\ -I_{xy} & I_{yy} & -I_{yz} \\ -I_{xz} & -I_{yz} & I_{zz} \end{bmatrix} \tag{11}$$

Define

$$H = \begin{bmatrix} 0 & h_z & -h_y \\ -h_z & 0 & h_x \\ h_y & -h_x & 0 \end{bmatrix} \tag{12a}$$

$$I_{\omega\omega} = \begin{bmatrix} (I_{zz} - I_{yy}) & I_{xy} & -I_{xz} \\ -I_{xy} & (I_{xx} - I_{zz}) & I_{yz} \\ I_{xz} & -I_{yz} & (I_{yy} - I_{xx}) \end{bmatrix} \tag{12b}$$

$$I_{\omega_2} = \begin{bmatrix} 0 & -I_{yz} & I_{yz} \\ I_{xz} & 0 & -I_{xz} \\ -I_{xy} & I_{xy} & 0 \end{bmatrix} \tag{12c}$$

$$\boldsymbol{\chi} = \begin{bmatrix} \omega_y \omega_z \\ \omega_x \omega_z \\ \omega_x \omega_y \end{bmatrix} \tag{12d}$$

$$\boldsymbol{\lambda} = \begin{bmatrix} \omega_x^2 \\ \omega_y^2 \\ \omega_z^2 \end{bmatrix} \tag{12e}$$

then Eq. (10) can be written as

$$\dot{\boldsymbol{\omega}} = -I^{-1}H\boldsymbol{\omega} - I^{-1}I_{\omega\omega}\boldsymbol{\chi} - I^{-1}I_{\omega_2}\boldsymbol{\lambda} + I^{-1}(\boldsymbol{T} - \dot{\boldsymbol{h}}) \tag{13}$$

Let

$$F_\omega = -I^{-1}H \tag{14a}$$

$$B_\omega = -I^{-1}I_{\omega\omega} \tag{14b}$$

$$B_{\omega_2} = -I^{-1}I_{\omega_2} \tag{14c}$$

$$\boldsymbol{f} = I^{-1}(\boldsymbol{T} - \dot{\boldsymbol{h}}) \tag{14d}$$

then Eq. (13) can be written as follows:

$$\dot{\boldsymbol{\omega}} = F_\omega\boldsymbol{\omega} + B_\omega\boldsymbol{\chi} + B_{\omega_2}\boldsymbol{\lambda} + \boldsymbol{f} \tag{15}$$

The latter is the desired rotational dynamics equation that expresses the time derivative of $\boldsymbol{\omega}$, the angular velocity vector of the SC with respect to inertial space, in terms of the known forcing function $\boldsymbol{f}$ and $\boldsymbol{\omega}$ itself. This equation is the central equation in the development of the filter.

We realize that the solution of Eq. (15) hinges on our knowledge of $\boldsymbol{\chi}$ and $\boldsymbol{\lambda}$. As will be shown later, they will be estimated by their own independent estimators. Those estimators will each need a dynamics model for the vector it is set to estimate. The derivation of these dynamics models is presented next.

First differentiate Eq. (12d) to obtain the dynamics equation

$$\dot{\chi} = \begin{bmatrix} \dot{\omega}_y\omega_z + \omega_y\dot{\omega}_z \\ \dot{\omega}_x\omega_z + \omega_x\dot{\omega}_z \\ \dot{\omega}_x\omega_y + \omega_x\dot{\omega}_y \end{bmatrix} \tag{16}$$

Let

$$F_\chi = 0 \tag{17a}$$

$$B_\chi = \begin{bmatrix} 0 & \dot{\omega}_z & \dot{\omega}_y \\ \dot{\omega}_z & 0 & \dot{\omega}_x \\ \dot{\omega}_y & \dot{\omega}_x & 0 \end{bmatrix} \tag{17b}$$

then Eq. (16) can be written as

$$\dot{\chi} = F_\chi\chi + B_\chi\omega \tag{18}$$

which is the desired dynamics equation for χ. To obtain the dynamics equation for λ differentiate Eq. (12e). This yields

$$\dot{\lambda} = \begin{bmatrix} 2\dot{\omega}_x & 0 & 0 \\ 0 & 2\dot{\omega}_y & 0 \\ 0 & 0 & 2\dot{\omega}_z \end{bmatrix} \begin{bmatrix} \omega_x \\ \omega_y \\ \omega_z \end{bmatrix} \tag{19}$$

Let

$$F_\lambda = 0 \tag{20a}$$

and

$$B_\lambda = \begin{bmatrix} 2\dot{\omega}_x & 0 & 0 \\ 0 & 2\dot{\omega}_y & 0 \\ 0 & 0 & 2\dot{\omega}_z \end{bmatrix} \tag{20b}$$

then Eq. (19) can written as

$$\dot{\lambda} = F_\lambda\lambda + B_\lambda\omega \tag{21}$$

Equations (15), (18), and (21) are the deterministic dynamics equations that describe the behavior in time of ω and the products of its components. They form the foundation of the stochastic dynamics model of the EIKF.

Next we develop the measurement equations that will serve as the basis of the stochastic measurement model used by the EIKF to update its estimates.

III. Measurement Equations

A. Raw Vector Measurements

We start by deriving the measurement equation for the primary KF whose dynamics is given in Eq. (15) and that estimates ω. Recall Eq. (2b) as

$$[\boldsymbol{b}\times]\omega = \dot{\boldsymbol{b}} - D_b^i\dot{\boldsymbol{b}}^i \tag{2b}$$

Let

$$z_{\omega b} = \dot{\boldsymbol{b}} - D_b^i\dot{\boldsymbol{b}}^i \tag{22a}$$

and

$$C_b = [\boldsymbol{b}\times] \tag{22b}$$

then Eq. (2b) can be rewritten as

$$z_{\omega b} = C_b\omega \tag{22c}$$

The measurement vector $z_{\omega b}$ is a computable three-dimensional vector, which is to be fed into the EIKF part that estimates ω.

We note that C_b is a 3×3 singular matrix. It is obvious that one of the three equations of Eq. (22c) is a linear combination of the other two and, thus, is superfluous. Although a white noise will be added to $z_{\omega b}$ at a later stage [see Eq. (37)] and, thus, will turn the three equations in Eq. (22c) into independent equations, the singularity of C_b will be troublesome. Problems may arise in the KF, designed to estimate ω, when computing its gain according to $K_\omega = P_\omega C_b^T[C_bP_\omega C_b^T + R_\omega]^{-1}$. The matrix $C_bP_\omega C_b^T$ is singular, and because the elements of the noise covariance matrix R_ω are rather small, the inverse yields a matrix whose elements are very large. This in turn yields a very inaccurate gain matrix. All that keeps the inverted matrix from being strictly singular is the noise covariance matrix. The physical meaning of this ill-conditioned case is that the noise is the added information that causes the dependent deterministic equations to be independent. This information is, of course, meaningless and should not be considered. As a remedy to this ill-conditioned case, we eliminate one of the rows of Eq. (22c). The question is then which row to eliminate. It is clear that the answer to this question hinges on the value of the components of $z_{\omega b}$. Obviously, if the SC rotates fast about the body z axis and not at all about the other two, then it can be seen either from Eq. (2b) or Eq. (22a) that the third component of $z_{\omega b}$ is negligible and, thus, the third row of Eq. (22c) should be eliminated. For the sake of the ensuing presentation we will assume that this is the case. This check, however, has to be performed before every measurement update of the filter. Having made the latter assumption, define

$$z'_{\omega b} = \begin{bmatrix} z_{\omega b,1} \\ z_{\omega b,2} \end{bmatrix} \tag{23a}$$

and

$$C'_b = \begin{bmatrix} 0 & -b_z & b_y \\ b_z & 0 & -b_x \end{bmatrix} \tag{23b}$$

then

$$z'_{\omega b} = C'_b\omega \tag{23c}$$

Next we develop the measurement equation needed to estimate χ and λ. We can choose one of two options, which are based on entirely different approaches. According to one approach we obtain the needed measurements from a second differentiation of a measured direction. It is well known,[8] and indeed very easily shown, that using the notation

$$\boldsymbol{w} = \dot{\boldsymbol{b}}^i \tag{24a}$$

and

$$\boldsymbol{u} = \dot{\boldsymbol{b}}^b \tag{24b}$$

the following holds:

$$D_b^i\dot{\boldsymbol{w}}^i = \dot{\boldsymbol{u}} + 2\omega\times\boldsymbol{u} + \dot{\omega}\times\boldsymbol{b} + \omega\times(\omega\times\boldsymbol{b}) \tag{25}$$

where $\dot{\boldsymbol{w}}^i$ is resolved in the i coordinates and, as before, the dot symbolizes time differentiation performed in the b coordinates. Let

$$z_{\chi\lambda b} = D_b^i\dot{\boldsymbol{w}}^i - \dot{\boldsymbol{u}} - 2\omega\times\boldsymbol{u} - \dot{\omega}\times\boldsymbol{b} \tag{26}$$

then Eq. (25) can be written as

$$z_{\chi\lambda b} = \omega\times(\omega\times\boldsymbol{b}) \tag{27a}$$

Let

$$M_b = \begin{bmatrix} 0 & b_z & b_y \\ b_z & 0 & b_x \\ b_y & b_x & 0 \end{bmatrix} \tag{27b}$$

$$N_b = \begin{bmatrix} 0 & -b_x & -b_x \\ -b_y & 0 & -b_y \\ -b_z & -b_z & 0 \end{bmatrix} \tag{27c}$$

then it can be easily verified that Eq. (27a) can be written as

$$z_{\chi\lambda b} = M_b\chi + N_b\lambda \tag{28}$$

Note that like z_ω before, $z_{\chi\lambda b}$ is a computable vector, which is information to be fed into the EIKF part that estimates χ and λ. Now,

the argument that led to the reduction of the expressions in Eq. (22) to the corresponding expression in Eq. (23) holds here, too. Consequently, we eliminate one row in the expressions in Eq. (27). (As before, the row to be eliminated is determined by the relative size of the components of $z_{\chi\lambda b}$.) Assume that the third row is eliminated, then if we define

$$z'_{\chi\lambda b} = \begin{bmatrix} z_{\chi\lambda b,1} \\ z_{\chi\lambda b,2} \end{bmatrix} \tag{29a}$$

$$M'_b = \begin{bmatrix} 0 & b_z & b_y \\ b_z & 0 & b_x \end{bmatrix} \tag{29b}$$

$$N'_b = \begin{bmatrix} 0 & -b_x & -b_x \\ -b_y & 0 & -b_y \end{bmatrix} \tag{29c}$$

it can be easily verified that Eq. (28) can be rewritten as

$$z'_{\chi\lambda b} = M'_b\boldsymbol{\chi} + N'_b\boldsymbol{\lambda} \tag{29d}$$

If we now have a second vector measurement, for example, $\boldsymbol{c}$, then we get an identical set of equations where now $\boldsymbol{b}$ is replaced by $\boldsymbol{c}$ and the subscript b is replaced by the subscript c. Explicitly, we do the following. Define

$$z_{\omega c} = \dot{\boldsymbol{c}} - D^i_b\dot{\boldsymbol{c}}^i \tag{30a}$$

and

$$C_c = [\boldsymbol{c}\times] \tag{30b}$$

$$\boldsymbol{m} = \dot{\boldsymbol{c}}^i \tag{30c}$$

$$\boldsymbol{n} = \dot{\boldsymbol{c}}^b \tag{30d}$$

$$z_{\chi\lambda c} = D^i_b\dot{\boldsymbol{m}}^i - \dot{\boldsymbol{n}} - 2\boldsymbol{\omega}\times\boldsymbol{n} - \dot{\boldsymbol{\omega}}\times\boldsymbol{c} \tag{30e}$$

$$M'_c = \begin{bmatrix} 0 & c_z & c_y \\ c_y & c_x & 0 \end{bmatrix} \tag{30f}$$

$$N'_c = \begin{bmatrix} 0 & -c_x & -c_x \\ -c_y & 0 & -c_y \end{bmatrix} \tag{30g}$$

then the measurement equations are

$$z'_{\omega c} = C'_c\boldsymbol{\omega} \tag{31a}$$

$$z'_{\chi\lambda c} = M'_c\boldsymbol{\chi} + N'_c\boldsymbol{\lambda} \tag{31b}$$

where the conversion of $z_{\omega c}$ to $z'_{\omega c}$ and C_c to C'_c is performed in a manner similar to that indicated in Eqs. (23a) and (23b) and similarly, the conversion of $z_{\chi\lambda c}$ to $z'_{\chi\lambda c}$ is according to the conversion shown in Eq. (29a). From the foregoing, the extension to the case where we have more than two vector measurements at one time point is obvious.

The other option for obtaining measurement equations needed to estimate $\boldsymbol{\chi}$ and $\boldsymbol{\lambda}$ is based on $\hat{\boldsymbol{\omega}}$, the EIKF-generated estimate of $\boldsymbol{\omega}$. We will postpone the introduction of this option until we present the EIKF.

B. Preprocessed Vector Measurements

When we measure two different vectors at the same time point, then, as shown in Eq. (8), we have enough equations to obtain an estimate of $\boldsymbol{\omega}$ without resorting to a recursive estimator. Therefore we can, first, compute an estimate of $\boldsymbol{\omega}$ using Eq. (8) and, then, filter the estimate using the EIKF. As mentioned before, this is what was basically done in Ref. 4, only that $\boldsymbol{\omega}$ was obtained as an output of gyroscopes rather than an analytic solution based on vector measurements. Although this approach does not fully utilize the capabilities of a recursive estimator, for the sake of completeness, we show here how to formulate the measurement equation to apply the EIKF in this case, too.

Recall Eq. (8)

$$\hat{\boldsymbol{\omega}} = G^{\#}\boldsymbol{d} \tag{8}$$

Let

$$z_{\omega p} = G^{\#}\boldsymbol{d} \tag{32}$$

and let U denote the 3×3 identity matrix; then we can write Eq. (22c) as

$$z_{\omega p} = U\boldsymbol{\omega} \tag{33}$$

The last equation is the measurement equation that corresponds to the dynamics equation (15).

The measurement equations for estimating $\boldsymbol{\chi}$ and $\boldsymbol{\lambda}$ can be either those presented in the preceding subsection, namely, Eq. (29d) and/or Eq. (31b), or they can be directly related to $\hat{\boldsymbol{\omega}}$ computed in Eq. (8). The latter will be explained subsequently when we introduce the suitable EIKF.

IV. EIKF Models

The dynamics and measurement equations presented in Secs. II and III, respectively, are nominal equations. In preparing the equations for use in a filtering routine, we add white noise vectors to them to express model uncertainties. These uncertainties stem from two sources: first, there are modeling errors because the equations are not the exact dynamics and measurement models and, second, in the suboptimal filter that we will use, we will assume that $\dot{\boldsymbol{\omega}}$ is constant in the propagation time interval that we will use to propagate the estimate of $\boldsymbol{\omega}$. This assumption is clearly an approximation, commonly used in nonlinear filtering, which yields satisfactory results. The importance of the white noise added to each dynamics equation is in its spectral density matrix, which we adjust by trial and error to obtain the best filter performance. Similarly, the white noise added to each of the measurement equations indicates the measurement accuracy expressed by the covariance matrix of the noise vectors. This covariance, too, is adjusted to yield the best filter performance. Adding $\boldsymbol{n}_\omega$ to the central dynamics model in Eq. (15) yields the following main dynamics model:

$$\dot{\boldsymbol{\omega}} = F_\omega\boldsymbol{\omega} + B_\omega\boldsymbol{\chi} + B_{\omega 2}\boldsymbol{\lambda} + \boldsymbol{f} + \boldsymbol{n}_\omega \tag{34}$$

Similarly, we add white noise vectors to the right-hand sides of Eqs. (18) and (21), which become

$$\dot{\boldsymbol{\chi}} = F_\chi\boldsymbol{\chi} + B_\chi\boldsymbol{\omega} + \boldsymbol{n}_\chi \tag{35}$$

$$\dot{\boldsymbol{\lambda}} = F_\lambda\boldsymbol{\lambda} + B_\lambda\boldsymbol{\omega} + \boldsymbol{n}_\lambda \tag{36}$$

Adding white noise vectors (of the appropriate dimensions) to the measurement equations turns Eqs. (23c), (29d), and (33), respectively, into

$$z'_{\omega b} = C'_b\boldsymbol{\omega} + \boldsymbol{v}'_{\omega b} \tag{37}$$

$$z'_{\chi\lambda b} = M'_b\boldsymbol{\chi} + N'_b\boldsymbol{\lambda} + \boldsymbol{v}'_{\chi\lambda b} \tag{38}$$

and

$$z_{\omega p} = U\omega + \boldsymbol{v}_\omega \tag{39}$$

The extension of Eqs. (37) and (38) to the case where we have more than one vector measurement is obvious.

As mentioned before, several measurement models that are based on the estimate of $\boldsymbol{\omega}$ will be introduced when we present the EIKF in the next section.

V. EIKF

Given the models of the preceding sections, we have several options for designing an EIKF. Like the models, the EIKF itself can be divided into two basic categories. The first category is one that handles raw vector measurements, and the second category is one which handles preprocessed vector measurements. In the ensuing, we only present the models to be used in the interlaced linear KFs. The KF algorithm itself can be found, of course, in standard KF texts (see, e.g., Ref. 3).

A. Raw Vector Measurements

We have several options for designing an EIKF when given raw vector measurements. Some options follow.

Option 1

We run three parallel linear KFs. The models used by the filters are as follows.

For filter 1 the dynamics model is given in Eq. (34), and the measurement equation is given in Eq. (37):

$$\dot{\boldsymbol{\omega}} = F_\omega \boldsymbol{\omega} + B_\omega \hat{\boldsymbol{\chi}} + B_{\omega 2} \hat{\boldsymbol{\lambda}} + \boldsymbol{f} + \boldsymbol{n}_\omega \tag{40a}$$

$$\boldsymbol{z}'_{\omega b} = C'_b \boldsymbol{\omega} + \boldsymbol{v}'_{\omega b} \tag{40b}$$

Note that $\hat{\boldsymbol{\chi}}$ and $\hat{\boldsymbol{\lambda}}$ are inputs from the other two filters that run in parallel to filter 1.

The dynamics model of the second filter is given in Eq. (35), and the measurement equation is derived from Eq. (38):

$$\dot{\boldsymbol{\chi}} = F_\chi \boldsymbol{\chi} + B_\chi \hat{\boldsymbol{\omega}} + \boldsymbol{n}_\chi \tag{41a}$$

$$\boldsymbol{z}'_{\chi\lambda b} - N'_b \hat{\boldsymbol{\lambda}} = M'_b \boldsymbol{\chi} + \boldsymbol{v}'_{\chi\lambda b} \tag{41b}$$

Here $\hat{\boldsymbol{\omega}}$ and $\hat{\boldsymbol{\lambda}}$ are inputs from the other two parallel filters.

The dynamics equation of the third filter is given in Eq. (36), and the measurement equation is derived from Eq. (38):

$$\dot{\boldsymbol{\lambda}} = F_\lambda \boldsymbol{\lambda} + B_\lambda \hat{\boldsymbol{\omega}} + \boldsymbol{n}_\lambda \tag{42a}$$

$$\boldsymbol{z}'_{\chi\lambda b} - M'_b \hat{\boldsymbol{\chi}} = N'_b \boldsymbol{\lambda} + \boldsymbol{v}'_{\chi\lambda b} \tag{42b}$$

Here $\hat{\boldsymbol{\omega}}$ and $\hat{\boldsymbol{\chi}}$ are inputs from the other two parallel filters.

Note that the preceding measurement equations are based on a single vector measurement, namely, $\boldsymbol{b}$. If we obtain another vector measurement, for example, $\boldsymbol{c}$, at a certain time point, then we use Eqs. (30) and (31) to generate measurement models similar to those given in Eqs. (40b), (41b), and (42b), and perform consecutive measurement updates of the three interlaced filters, or we can augment the two vector measurements in each filter and in each of them perform one combined measurement update at that time point. The extension of this case to more than two simultaneous measurements is immediate. The three-filter model of option 1 is summarized in Table 1. A block diagram representation of the EIKF of option 1 is shown in Fig. 1.

Option 2

Here we run only two parallel interlaced linear KF. They are as follows.

Table 1 Filter model of option 1

Dynamics	Equation	Measurement	Equation
$\dot{\boldsymbol{\omega}} = F_\omega \boldsymbol{\omega} + B_\omega \hat{\boldsymbol{\chi}} + B_{\omega 2} \hat{\boldsymbol{\lambda}} + \boldsymbol{f} + \boldsymbol{n}_\omega$	(40a)	$\boldsymbol{z}'_{\omega b} = C'_b \boldsymbol{\omega} + \boldsymbol{v}'_{\omega b}$	(40b)
$\dot{\boldsymbol{\chi}} = F_\chi \boldsymbol{\chi} + B_\chi \hat{\boldsymbol{\omega}} + \boldsymbol{n}_\chi$	(41a)	$\boldsymbol{z}'_{\chi\lambda b} - N'_b \hat{\boldsymbol{\lambda}} = M'_b \boldsymbol{\chi} + \boldsymbol{v}'_{\chi\lambda b}$	(41b)
$\dot{\boldsymbol{\lambda}} = F_\lambda \boldsymbol{\lambda} + B_\lambda \hat{\boldsymbol{\omega}} + \boldsymbol{n}_\lambda$	(42a)	$\boldsymbol{z}'_{\chi\lambda b} - M'_b \hat{\boldsymbol{\chi}} = N'_b \boldsymbol{\lambda} + \boldsymbol{v}'_{\chi\lambda b}$	(42b)

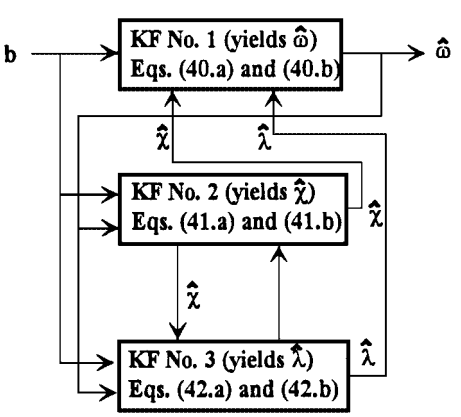

Fig. 1 Block diagram representation of the EIKF of option 1.

Filter 1 of option 2 is identical to filter 1 of option 1.

To present filter 2, we adopt the following definitions:

$$\boldsymbol{X} = \begin{bmatrix} \boldsymbol{\chi} \\ \boldsymbol{\lambda} \end{bmatrix} \tag{43a}$$

$$F_x = \begin{bmatrix} F_\chi & 0 \\ 0 & F_\lambda \end{bmatrix} \tag{43b}$$

$$B_x = \begin{bmatrix} B_\chi \\ B_\lambda \end{bmatrix} \tag{43c}$$

$$\boldsymbol{n}_x = \begin{bmatrix} \boldsymbol{n}_\chi \\ \boldsymbol{n}_\lambda \end{bmatrix} \tag{43d}$$

$$\boldsymbol{z}'_{xb} = \boldsymbol{z}'_{\chi\lambda b} \tag{44a}$$

$$C'_{xb} = [M'_b \quad N'_b] \tag{44b}$$

$$\boldsymbol{v}'_{xb} = \boldsymbol{v}'_{\chi\lambda b} \tag{44c}$$

then Eqs. (41a) and (42a) can be augmented into the single dynamics equation

$$\dot{\boldsymbol{X}} = F_x \boldsymbol{X} + B_x \hat{\boldsymbol{\omega}} + \boldsymbol{n}_x \tag{45a}$$

and Eq. (38) can be written to suit Eq. (45a) as

$$\boldsymbol{z}'_{xb} = C'_{xb} \boldsymbol{X} + \boldsymbol{v}'_{xb} \tag{45b}$$

The EIKF model of option 2 is summarized in Table 2. A block diagram representation of this EIKF is shown in Fig. 2.

Option 3

Recall that in option 1, as well as in option 2, we had to use the second time derivative of the measured vectors to generate the data for the measurement models. We can use a different approach, though, that does not require a second differentiation. We simply use $\hat{\boldsymbol{\omega}}$, which is estimated in filter 1 and treat it in the other parallel filters as a measurement of $\boldsymbol{\chi}$ and $\boldsymbol{\lambda}$ because they are functions of $\boldsymbol{\omega}$ [see Eqs. (12d) and (12e)]. Doing so we obtain the following measurement equations:

$$\begin{bmatrix} \hat{\omega}_y \hat{\omega}_z \\ \hat{\omega}_x \hat{\omega}_z \\ \hat{\omega}_x \hat{\omega}_y \end{bmatrix} = \begin{bmatrix} 1 & 0 & 0 \\ 0 & 1 & 0 \\ 0 & 0 & 1 \end{bmatrix} \begin{bmatrix} \omega_y \omega_z \\ \omega_x \omega_z \\ \omega_x \omega_y \end{bmatrix} + \begin{bmatrix} v_{\chi x} \\ v_{\chi y} \\ v_{\chi z} \end{bmatrix} \tag{46}$$

which we can write as

$$\boldsymbol{z}_\chi = U \boldsymbol{\chi} + \boldsymbol{v}_\chi \tag{47a}$$

In a similar manner we obtain

$$\boldsymbol{z}_\lambda = U \boldsymbol{\lambda} + \boldsymbol{v}_\lambda \tag{47b}$$

Table 2 Filter model of option 2

Dynamics	Equation	Measurement	Equation
$\dot{\boldsymbol{\omega}} = F_\omega \boldsymbol{\omega} + B_\omega \hat{\boldsymbol{\chi}} + B_{\omega 2} \hat{\boldsymbol{\lambda}} + \boldsymbol{f} + \boldsymbol{n}_\omega$	(40a)	$\boldsymbol{z}'_{\omega b} = C'_b \boldsymbol{\omega} + \boldsymbol{v}'_{\omega b}$	(40b)
$\dot{\boldsymbol{X}} = F_x \boldsymbol{X} + B_x \hat{\boldsymbol{\omega}} + \boldsymbol{n}_x$	(45a)	$\boldsymbol{z}'_{xb} = C'_{xb} \boldsymbol{X} + \boldsymbol{v}'_{xb}$	(45b)

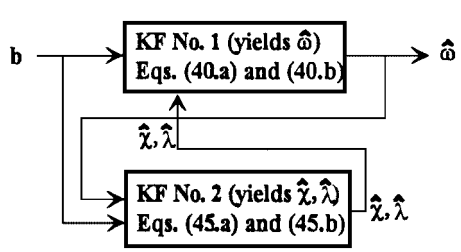

Fig. 2 Block diagram representation of the EIKF of option 2.

Table 3 Filter model of option 3

Dynamics	Equation	Measurement	Equation
$\dot{\omega} = F_\omega \omega + B_\omega \hat{\chi} + B_{\omega 2}\hat{\lambda} + f + n_\omega$	(40a)	$z'_{\omega b} = C'_b \omega + v_{\omega b}$	(40b)
$\dot{\chi} = F_\chi \chi + B_\chi \hat{\omega} + n_\chi$	(41a)	$z_\chi = U\chi + v_\chi$	(47a)
$\dot{\lambda} = F_\lambda \lambda + B_\lambda \hat{\omega} + n_\lambda$	(42a)	$z_\lambda = U\lambda + v_\lambda$	(47b)

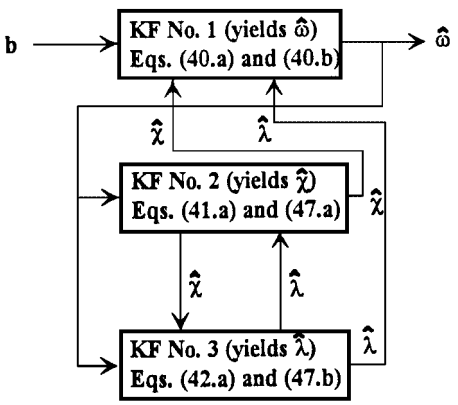

Fig. 3 Block diagram representation of the EIKF of option 3.

where, as before, U is the identity matrix. We add the white noise vectors v_χ and v_λ because on the left-hand side of Eq. (47) we do not have χ and λ but rather their estimates. In this option the three parallel filters are as follows.

Filter 1 of option 3 is identical to filter 1 in option 1.

The dynamics equation filter 2 is exactly like the one given in Eq. (41a), but the measurement equation is that given in Eq. (47a); that is,

$$\dot{\chi} = F_\chi \chi + B_\chi \hat{\omega} + n_\chi \tag{41a}$$

$$z_\chi = U\chi + v_\chi \tag{47a}$$

The dynamics equation filter 3 is exactly like the one given in Eq. (42a), but the measurement equation is that given in Eq. (47b); that is,

$$\dot{\lambda} = F_\lambda \lambda + B_\lambda \hat{\omega} + n_\lambda \tag{42a}$$

$$z_\lambda = U\lambda + v_\lambda \tag{47b}$$

The EIKF model of option 3 is summarized in Table 3. A block diagram representation of the EIKF of option 3 is shown in Fig. 3.

B. Preprocessed Vector Measurements and EIKF

As we have already seen, preprocessed vector measurements yield an estimate of ω, and as mentioned earlier, the full advantage of a recursive estimator is not utilized when a measurement or an estimate of ω is available; however, for the sake of completeness, we present an EIKF scheme for this case, too.

The filter model of this case is similar to the model of option 3. The dynamics equation of the present filter 1 is identical to that of option 3 but the measurement equation is different. Now the measurements that are fed into filter 1 are not vector measurements, but rather a preliminary estimate of ω, which we denote by $\hat{\omega}_p$; thus, following Eqs. (8) and (32) we define

$$\hat{\omega}_p = G^{\#} d \tag{48a}$$

and

$$z_{\omega p} = \hat{\omega}_p \tag{48b}$$

and then, following Eq. (39), we write the measurement equation of filter 1 as

$$z_{\omega p} = U\omega + v_\omega \tag{48c}$$

Table 4 Model of the EIKF for preprocessed vector measurements

Dynamics	Equation	Measurement	Equation
$\dot{\omega} = F_\omega \omega + B_\omega \hat{\chi} + B_{\omega 2}\hat{\lambda} + f + n_\omega$	(40a)	$z_{\omega p} = U\omega + v_\omega$	(48c)
$\dot{\chi} = F_\chi \chi + B_\chi \hat{\omega} + n_\chi$	(41a)	$z_{\chi p} = U\chi + v_{\chi p}$	(49b)
$\dot{\lambda} = F_\lambda \lambda + B_\lambda \hat{\omega} + n_\lambda$	(42a)	$z_{\lambda p} = U\lambda + v_{\lambda p}$	(50b)

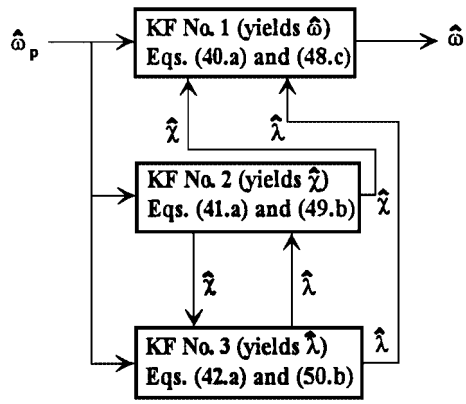

Fig. 4 Block diagram representation of the EIKF for preprocessed vector measurements.

As for filters 2 and 3, although their dynamics equations are identical to those of option 3, their measurement equations can be based on either the input $\hat{\omega}_p$ (which is also the input to the present filter 1), or on $\hat{\omega}$ (which is the input to filters 2 and 3 of option 3). The EIKF of this case is as follows.

We run three linear filters in parallel.

For filter 1 the dynamics equation is identical to that of option 3. The measurement equation is

$$z_{\omega p} = U\omega + v_\omega \tag{48c}$$

For filter 2 the dynamics model is identical to that of filter 2 of option 3. As for the measurement model, define

$$z_{\chi p} = \begin{bmatrix} \hat{\omega}_{py}\hat{\omega}_{pz} \\ \hat{\omega}_{px}\hat{\omega}_{pz} \\ \hat{\omega}_{px}\hat{\omega}_{py} \end{bmatrix} \tag{49a}$$

then

$$z_{\chi p} = U\chi + v_{\chi p} \tag{49b}$$

For filter 3 the dynamics model is identical to that of filter 3 of option 3. As for the measurement model, define

$$z_{\lambda p} = \begin{bmatrix} \hat{\omega}^2_{px} \\ \hat{\omega}^2_{py} \\ \hat{\omega}^2_{pz} \end{bmatrix} \tag{50a}$$

then

$$z_{\lambda p} = U\lambda + v_{\lambda p} \tag{50b}$$

The model of the EIKF for the preprocessed vector measurements is summarized in Table 4. A block diagram representation of the latter EIKF is shown in Fig. 4. As mentioned earlier, here, too, we have several options. We can, for example, use $\hat{\omega}_p$ in the dynamics equation of filters 2 and 3 in addition to using it as measurements in these two filters.

VI. Filter Testing

Option 1 (see Table 1 and Fig. 1) was chosen to be implemented. After obtaining satisfactory results with simulated telemetry, real magnetometer data (b_i) and sun sensor data (c_i) from the Rossi X-Ray Timing Explore (RXTE) satellite, which was launched on Dec. 30, 1995, were used. We chose a segment of data starting

Jan. 4, 1996, at 21 h, 43 min, and 31.148 s, which preceded a body z-axis maneuver that occurred 288 s into the data. The true rate obtained from the RXTE gyros and the estimated rate about the body axes are shown in Fig. 5. (The attitude of RXTE is determined onboard using gyros and star stackers.) It can be observed that during the maneuver the estimated rates followed the true rates but with a significant error. However, the rate estimation error decreased considerably at 204 s (t_1) into the maneuver (492 s from the start of the data). From that point on, the x and y estimation errors remained small, whereas the z component started to grow larger. The reasons for these phenomena are as follows. Up until t_1, there were no sun sensor measurements, and the rate estimation relied solely on the dynamics and the magnetometer measurements of the Earth magnetic field. At t_1, the sun sensor data were acquired, and they, along with the magnetometer data, were used by the EIKF. However, the sun direction was very nearly collinear with the spacecraft z axis. In fact, at t_1 the separation between the sun vector and the z axis was only 0.055 deg, and it decreased to 0.01 deg by the end of the maneuver. Because the magnetometer measurement of the Earth magnetic field vector was some 60 deg from the body z axis, there was no observability problem about the z axis. However, because the magnetometers are 30 times less accurate than the sun sensor, the z-axis rate estimate was corrupted. This corruption increased as the sun vector became more collinear with the body z axis. At the same time, the sun sensor measurements provided plenty of information on the x and y body rates. Thus, in contrast to the z-axis rate estimation error, the x and y rate estimation errors stayed small.

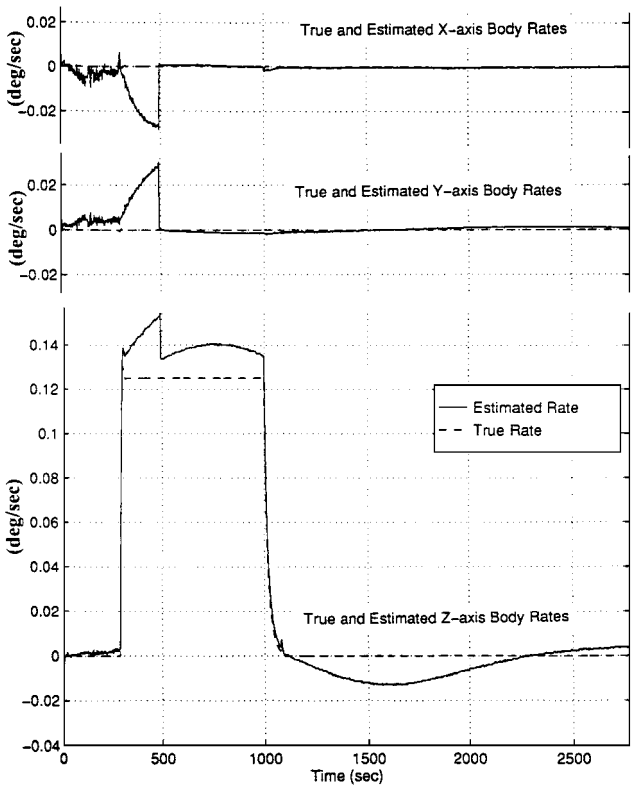

Fig. 5 True and estimated body rates.

The yaw rate estimation problem just described can be overcome by the generation of a so-called companion vector (CV), which is the vector formed from the cross product of the magnetometer and sun sensor measurements. Once formed, the CV is used in the EIKF as an additional measurement. The only difference between using the sensor measurements and the CV is the off diagonal elements in the R matrix, which can be easily computed. The true and estimated rates using the CV are presented in Fig. 6. When comparing Fig. 6 to Fig. 5 it is observed that, indeed, once sun sensor measurements are available (from t_1 on), the complete attitude is available via the CV and its derivative and the magnetometer measurements. As a result, the errors are reduced, particularly in the z component.

The CV can be used only when the sun sensor data is available, that is, from time t_1 and on. The rate estimation inaccuracy, which occurs in the lack of sun sensor measurements ($t < t_1$), can be mitigated by the generation of the so-called self-vector (SV), which like the CV serves as another pair of corresponding vector measurements as described in Sec. III.A. The SV is formed from the cross product of the measured magnetic field vector at time $(t - \Delta t)$ with the measured magnetic field vector at time t. Figure 7 presents the true and estimated rate components when both the SV and CV were

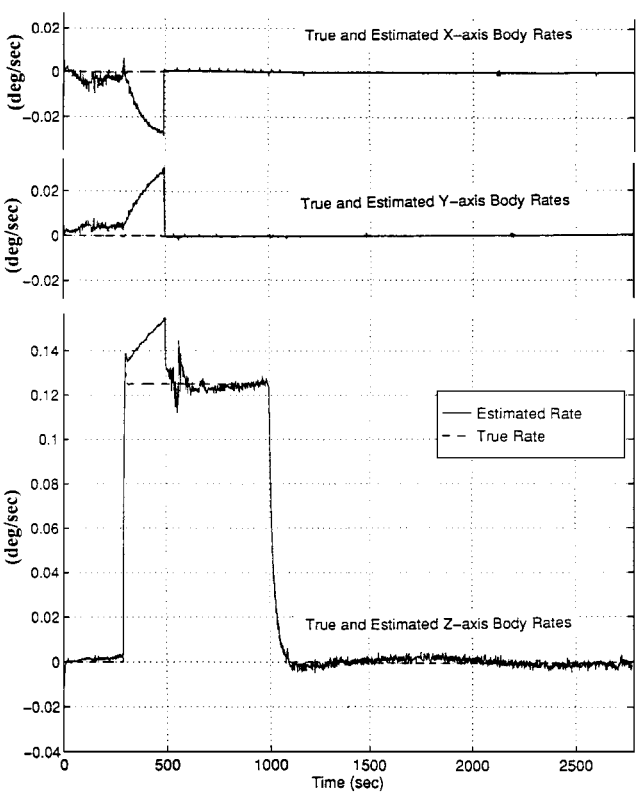

Fig. 6 True and estimated body rates when the CV is used as added measurement.

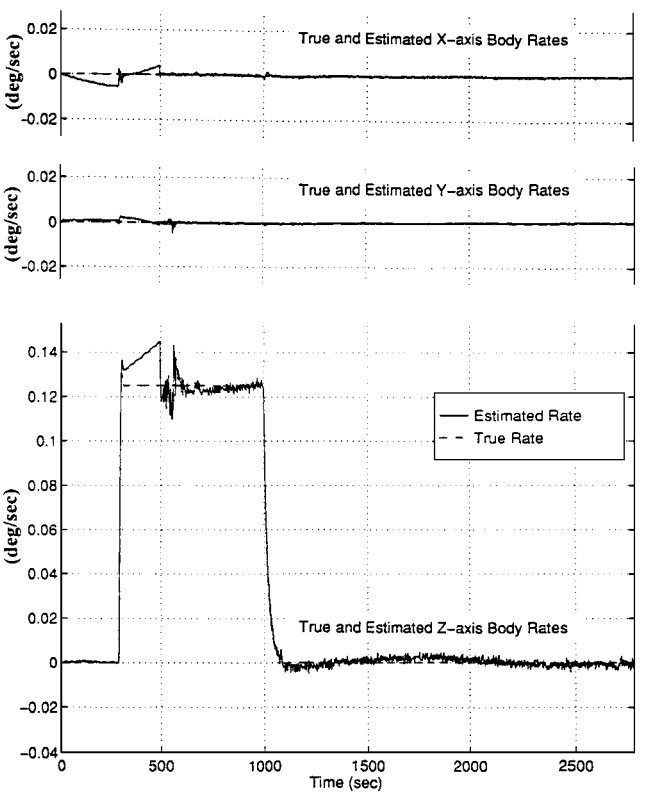

Fig. 7 True and estimated angular rate components when both the SV and CV are used as added measurements.

used as added measurements. The SV was added (to the magnetometer measurements) only during the time interval $0 \leq t \leq t_1$ when no sun sensor data existed, and after the acquisition of sun sensor data only the CV was added (to the sun sensor and magnetometer measurements). A comparison between Figs. 6 and 7 reveals that, indeed, the errors during the time interval $0 \leq t \leq t_1$ are smaller, in particular in the x and y components. A slight reduction also is observed in the peak error of the z component.

VII. Conclusions

We presented an algorithm for estimating the angular velocity of a rigid body such as a satellite. The algorithm is based on vector measurements and their derivatives. This algorithm is an extension of the IKF estimator, which was introduced in the past by Algrain and Saniie.[4] The IKF enables the use of several linear filters running in parallel for estimating the state of a nonlinear dynamic system. We developed an IKF for a more general dynamic model, the EIKF. Unlike Algrain and Saniie, who use angular velocity, we use direction vectors (such as sun, nadir, and star directions) or the magnetic field vector to obtain an estimate of the angular velocity. This is a more efficient use of the estimator. We presented several versions of the EIKF for angular velocity estimation.

The EIKF algorithm was tested using real RXTE satellite data for estimating its angular velocity vector. Magnetometer and sun sensor measurements were used. The results indicate that the algorithm performs very well. It was found that even when the measurements of only one spatially varying vector are available (in this case the Earth magnetic field), the algorithm still yields reasonable results. The RXTE measurements that were used in the testing had two shortcomings, namely, the lack of sun sensor data until the middle of the yaw maneuver and the near collinearity of the sun vector and the body z axis. Thus, the rate estimation about the z axis relies on the inaccurate magnetometer measurements even after the availability of the sun sensor data. Two solutions to these problems were suggested, tested, and proven to have solved the problem. In conclusion, the performance of the EIKF for estimating the angular velocity of a rigid body based on its dynamics model and on the measurements of two vectors that are not collinear was found to be very reasonable.

Acknowledgment

A part of this work was supported by a National Research Council–NASA Goddard Space Flight Center Research Fellowship.

References

[1] Natanson, G., "A Deterministic Method for Estimating Attitude from Magnetometer Data Only," *Proceedings of the 43rd International Astronautical Federation Congress*, Paper IFA-92-0036, Washington, DC, Aug.–Sept. 1992.

[2] Challa, M., Natanson, G., Deutschmann, J., and Galal, K., "A PC-Based Magnetometer-Only Attitude and Rate Determination System for Gyroless Spacecraft," *Proceedings of the Flight Mechanics/Estimation Theory Symposium*, NASA Goddard Space Flight Center, 1995, pp. 83–96.

[3] Gelb, A. (ed.), *Applied Optimal Estimation*, MIT Press, Cambridge, MA, 1974, p. 19.

[4] Algrain, M. C., and Saniie, J., "Interlaced Kalman Filtering of 3-D Angular Motion Based on Euler's Nonlinear Equations," *IEEE Transactions on Aerospace and Electronic Systems*, Vol. 30, No. 1, 1994, pp. 175–185.

[5] Algrain, M. C., and Ehlers, D., "Novel Kalman Filtering Method for Suppression of Gyroscope Noise Effects in Pointing and Tracking Systems," *Optical Engineering*, Vol. 34, No. 10, 1995.

[6] Wertz, J. R. (ed.), *Spacecraft Attitude Dynamics and Control*, Reidel, Dordrecht, The Netherlands, 1984, p. 523.

[7] Agrawal, B. N., *Design of Geosynchronous Spacecraft*, Prentice–Hall, Englewood Cliffs, NJ, 1986, p. 109.

[8] Meriam, J. L., and Kraige, L. G., *Engineering Mechanics. Volume 2, Dynamics*, Wiley, New York, 1992, pp. 383–386.